Detonation Initiation in Tube by Coaxial Predetonator

Hirokazu Nishimura, Takuya Matsumura, Yutaka Koga, Tomoaki Yatsufusa, Takuma Endo, and Shiro Taki

Department of Mechanical Engineering, Hiroshima University
Higashi-Hiroshima, 739-8527 Japan

1 Introduction

Pulse detonation engines (PDEs) are now under development not only as propulsion devices [1] but also as power generators [2]. One of key issues in the PDE development is to make the operation frequency higher. However, the deflagration-to-detonation transition in hydrocarbon-air mixtures needs long distance and time even if Shchelkin spiral and/or perforated plates are used [3]. At the present stage, a predetonator, which is a small chamber charged with a highly detonable mixture and connected to the main combustor to help the detonation initiation there, seems one of the hopeful candidates for the effective detonation-initiation device. The most important requirement for a predetonator is to initiate detonations in the main combustor reliably.

In the present paper, we report the results of fundamental experiments on coaxial predetonators. Particularly, the critical conditions for the predetonators to initiate detonations in the main combustor (detonation tube) and the behavior of the detonation cell structure in the detonation-initiation phase were investigated in detail.

2 Experimental Arrangement

Figure 1 shows the experimental arrangement. The experiments were carried out using a cylindrical tube of 2035 mm in length and 100 mm in inner diameter as the main combustor, which is called the detonation tube hereafter. The predetonators, which were cylindrical tubes of 44.5 mm and 30 mm in inner diameter (D_{PD}), were coaxially connected to the detonation tube. The length of the predetonators was varied by combining several tubes, whose lengths were 200, 300, 400, and 800 mm (D_{PD}=44.5 mm), or 400 and 800 mm (D_{PD}=30 mm). The total length of the predetonators further included a connection flange whose thickness was 30 mm. A diaphragm of polymer film whose thickness was 100 μm isolated the detonation tube from the predetonator. A connection flange whose thickness was 25 mm was inserted between the diaphragm and the detonation tube. The gas mixture in the predetonator was ignited by an automotive spark plug. In order to confirm the detonation propagation in the predetonator, a pressure transducer (PT) and an ion probe (I0) were installed on the side wall of the predetonator. For the investigation of the detonation initiation in the detonation tube, ion probes (I1 and I3) and soot foils were installed on the side wall of the detonation tube. The soot foils were of stainless steel and of 0.2 mm in thickness. By the ion probes and the soot foils, the propagation speed of the flame in the laboratory system and the detonation cell structure were obtained, respectively.

The gas mixtures we investigated in the detonation tube were C_3H_8+5(O_2+3.76βN_2), C_3H_8+5(O_2+3.76βAr), and $2H_2$+(O_2+3.76βN_2) at the ambient conditions of temperature and pressure, where β was the parameter representing the dilution ratio. The predetonator was filled with the stoichiometric C_3H_8-O_2 gas mixture at room temperature in all cases. The length and the initial gas pressure of the predetonator were varied as the governing

Correspondence to : nishimura-joy@hiroshima-u.ac.jp

parameters. Although the stoichiometric C_3H_8-O_2 gas mixture was mixed in the predetonator, the investigated gas mixtures filling the detonation tube were premixed in another tank with a stirrer.

The size of each soot foil was 300 mm in width and 400 mm in length, and five soot foils were installed on the side wall of the detonation tube. Figure 2 shows an example of the soot-foil record. This shows the first and second soot foils from the predetonator side. The X coordinate is set as shown in Fig. 2, where the left edge of the first soot foil, located at 25 mm from the diaphragm, corresponds to X=0. The leading edge of the detonation cell structure is denoted by X_0. We measured the cell width at equally-spaced locations from X_0.

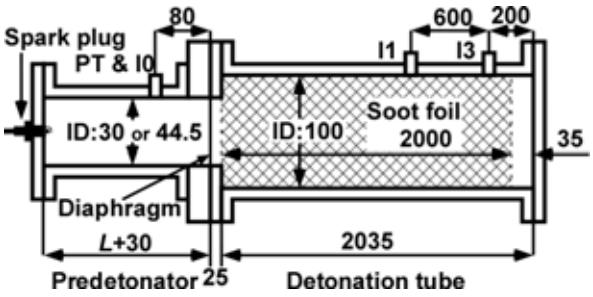

Fig. 1 Experimental arrangement (in mm).

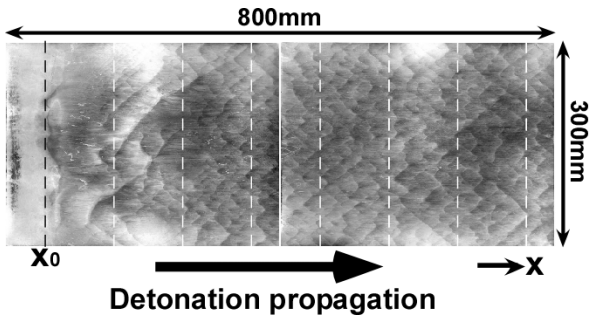

Fig. 2 Soot foil record (C_3H_8:O_2:N_2=1:5:13.2).

3 Results and Discussions

3.1 Predominant governing parameter for the detonation initiation

In order to clarify the predominant governing parameter of the predetonator for the detonation initiation in the detonation tube, we carried out experiments using C_3H_8+5(O_2+3.76βN_2) gas mixture with β=1.0 varying the length and the initial gas pressure of the predetonator whose inner diameter was 44.5 mm. The initial gas pressure of the predetonator was varied in the range of 50-130 kPa because detonations were not reliably initiated in the predetonator when it was lower than 50 kPa. Figure 3 summarizes the experimental results, where Q_{PD} denotes the total released heat in the predetonator, which was evaluated by using the lower heating value of propane, and P_{PD} denotes the initial gas pressure of the predetonator. The closed and open circles show the conditions for successful and unsuccessful detonation initiation in the detonation tube, respectively. As shown in Fig. 3, Q_{PD} was the predominant governing parameter for the detonation initiation in the detonation tube although its critical value slightly depended on P_{PD}. We call the critical value of Q_{PD} for the detonation initiation in the detonation tube the critical initiation energy (Q_{cr}) hereafter, and it was about 12 kJ in this case.

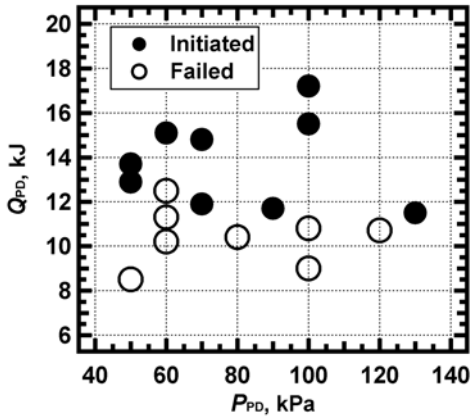

Fig. 3 Influence of Q_{PD} and P_{PD} on the detonation initiation in the detonation tube.

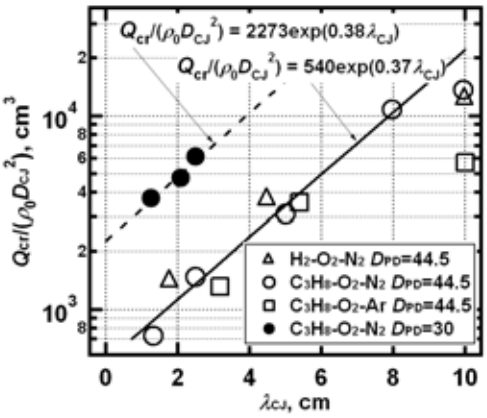

Fig. 4 The dependence of Q_{cr} on λ_{CJ}.

3.2 Dependence of the critical initiation energy on the cell width

The values of Q_{cr} were experimentally determined. In the experiments where the 44.5-mm predetonator was used, the investigated gas mixtures were $C_3H_8+5(O_2+3.76\beta N_2)$, $C_3H_8+5(O_2+3.76\beta Ar)$, and $2H_2+(O_2+3.76\beta N_2)$, β was varied in the range of 0.5-4.5, and P_{PD} was varied in the range of 50-180 kPa. On the other hand, in the experiments where the 30-mm predetonator was used, the investigated gas mixture was $C_3H_8+5(O_2+3.76\beta N_2)$, β was varied in the range of 0.5-0.7, and P_{PD} was varied in the range of 100-210 kPa. And for each gas mixture, we measured the cell width of the steady detonation propagating at the Chapman-Jouguet (CJ) detonation speed. Figure 4 shows the experimental results in terms of λ_{CJ} that denotes the cell width of the steady detonation. The vertical axis denotes the modified critical initiation energy $Q_{cr}/(\rho_0 D_{CJ}^2)$. In the vicinity of the propagation limit, namely, in the cases where λ_{CJ} became close to the tube diameter (100 mm), the critical initiation energy Q_{cr} seemed to become smaller in comparison with the cases where λ_{CJ} were small enough against the tube diameter. This might be due to the coupling between a detonation wave and downstream acoustic field, which is shown in spinning detonations. In Fig. 4, the solid line was obtained by fitting the data for the 44.5-mm predetonator in the range that λ_{CJ} was smaller than 100 mm, and the broken line was obtained by fitting the data for the 30-mm predetonator.

3.3 Behavior of the detonation cell structure in the initiation phase

In order to study the initiation process of detonation, we investigated the behavior of the detonation cell structure. The gas mixtures we used were $C_3H_8+5(O_2+3.76\beta N_2)$ where β was 0.7 or 1.0, and the 44.5-mm predetonator was used. Table 1 shows some measured values of X_0. When the detonation initiation was unsuccessful, the soot on the entire area of the soot foils was removed. When the detonation initiation was successful, the soot was removed in the leading portion, whose width was X_0, of the foil, and the detonation cell structure was observed in the region $X>X_0$. As shown in Table 1, X_0 was almost constant in the present experiments. Therefore, X_0 may be determined predominantly by the geometrical configuration, that is, the diameters of the predetonator and the detonation tube.

Table 1 Measured values of X_0

β	Q_{PD} [kJ]	X_0 [mm]
0.7	4.8	Failed.
0.7	6.9	79
0.7	51.4	68
1	9	Failed.
1	15.5	68
1	26.1	78
1	51.7	68

Figure 5 shows the evolution of the cell width along propagation, where L_{CJ} denotes the cell length of the steady detonation. When Q_{PD} was much larger than Q_{cr} (typically, $Q_{PD}/Q_{cr} \geq 4$), the cell width (λ) was initially much smaller than λ_{CJ}, became larger along propagation, and finally, coincided with λ_{CJ} asymptotically. When $Q_{PD}/Q_{cr} \approx 2$, the initial cell width was close to λ_{CJ}, became a little smaller once, and finally, coincided with λ_{CJ} asymptotically. When Q_{PD} was a little larger than Q_{cr}, the initial cell width was much larger than λ_{CJ}, became close to λ_{CJ} at about $(X-X_0)/L_{CJ} \approx 7$, and finally, coincided with λ_{CJ} asymptotically. Especially, the case where β=0.7 and Q_{PD}=6.9 kJ was remarkable. Figure 6 shows the initial portion (800 mm) of the soot-foil record obtained in this case. At about X=40 mm, a micro-explosion occurred on the side wall of the detonation tube. Although this initial micro-explosion seemed to be triggered by disturbances arisen from the seam of the soot foil, this did not seem essential because a detonation was successfully initiated without a soot foil in the case where β=0.7 and Q_{PD}=6.4 kJ. This initial micro-explosion generated two transverse waves propagating along the leading shock front in opposite directions, and these transverse waves collided at about X=120 mm (the value of X_0 was evaluated as the average of the location where the initial micro-explosion occurred and that where the initial two transverse waves collided), and after this transverse-wave collision, many transverse waves were

rapidly generated at about X=250 mm. This is why the cell width became small rapidly between $(X-X_0)/L_{CJ}$=5 and 7 in the case where β=0.7 and Q_{PD}=6.9 kJ. Finally, the cell width converged to its steady value at $(X-X_0)/L_{CJ}$=10-15 in all cases when detonation was successfully initiated.

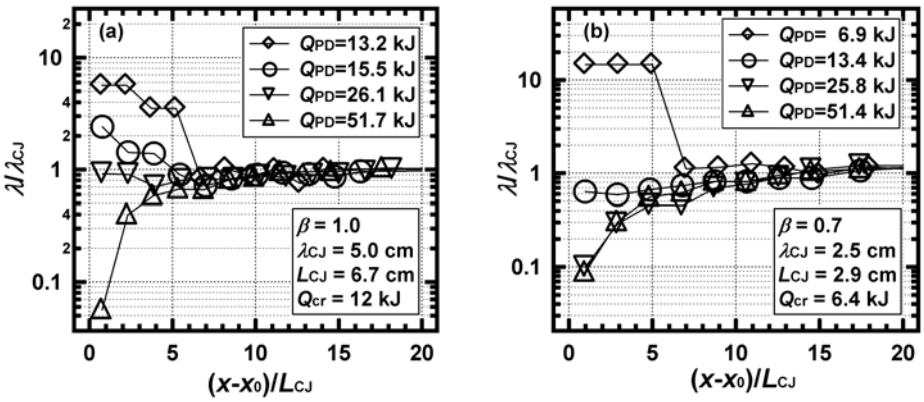

Fig. 5 Evolution of the detonation cell width.

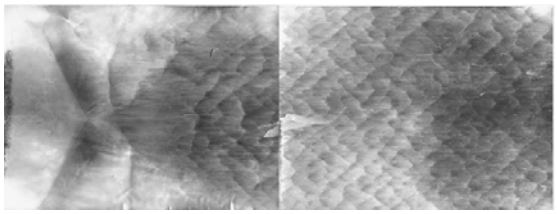

Fig. 6 Soot-foil record (C_3H_8-O_2-N_2 mixture, β=0.7, Q_{PD}=6.9 kJ, 300×800 mm)

4 Conclusions

We carried out fundamental experiments on coaxial-type predetonator for application to pulse detonation engines. Particularly, the critical conditions for the predetonator to initiate a detonation in the main combustor (detonation tube) and the behavior of the detonation cell structure in the detonation-initiation phase were investigated in detail. The detonable gases we investigated were stoichiometric C_3H_8-O_2-N_2, C_3H_8-O_2-Ar, and H_2-O_2-N_2 mixtures at the room temperature and 100 kPa in pressure. The predetonator was filled with the stoichiometric C_3H_8-O_2 gas mixture in all cases. It was found that the predominant governing parameter for the detonation initiation in the detonation tube was the total released heat in the predetonator. Its critical value for the detonation initiation in the detonation tube (Q_{cr}) was roughly scaled as $\exp(0.4\lambda_{CJ})$, where λ_{CJ} denotes the cell width of the steady detonation propagating at the Chapman-Jouguet (CJ) detonation speed.

References

[1] Roy, G. D., Frolov, S. M., Borisov, A. A., and Netzer, D. W., Pulse detonation propulsion: challenges, current status, and future perspective. Progress in Energy and Combustion Science 30: 545-672 (2004)

[2] Endo, T., Yatsufusa, T., Taki, S., and Kasahara, J., Thermodynamic analysis of the performance of a pulse detonation turbine engine (in Japanese). Science and Technology of Energetic Materials 65: 103-110 (2004)

[3] Sorin, R., Zitoun, R., and Desbordes, D., Optimization of the deflagration to detonation transition: reduction of length and time of transition. Shock Waves 15: 137-145 (2006)